Environmental Science and Pollution Research (2020) 27:3962–3978
https://doi.org/10.1007/s11356-019-06955-5

RESEARCH ARTICLE

Assessment of iron-modified calcite/zeolite mixture as a capping material to control sedimentary phosphorus and nitrogen liberation

Yanhui Zhan[1] · Yang Yu[1] · Jianwei Lin[1] · Xiaolong Wu[1] · Yan Wang[1] · Yuying Zhao[1]

Received: 25 June 2019 / Accepted: 4 November 2019 / Published online: 10 December 2019

Abstract

Calcite/zeolite mixture (CZ) can be used to construct a capping layer for the simultaneous management of phosphorus (P) and nitrogen (N) liberation from sediments into the overlying water (OVER-water). However, its control efficiency of sedimentary P release still needs to be improved. To address this issue, an iron-modified CZ (Fe-CZ) was synthesized, characterized, and employed as a capping material to simultaneously prevent P and N release from sediments into OVER-water. Batch and microcosm incubation experiments were performed to study the efficiency and mechanism for the control of P and N release from sediments by capping Fe-CZ. Results showed that sediment capping with Fe-CZ resulted in the significant reduction of soluble reactive P (SRP) and ammonium-N (NH_3-N) in OVER-water, with reduction rates of 77.8–99.7% and 54.0–96.7%, respectively. Furthermore, the Fe-CZ capping layer decreased the SRP concentration in the pore water (PORE-water) at depth of 0–30 mm and reduced the concentration of PORE-water NH_3-N at depth of 0–50 mm. Moreover, the Fe-CZ capping layer gave rise to the great decrement of the concentration of the labile P measured by DGT (diffusive gradient in thin films) technology (P-DGT) in the profile of OVER-water and sediment. Additionally, the Fe-CZ capping resulted in the reduction of redox-sensitive P (P-BD) in the 0–50 mm sediment and caused the transformation of P-BD to calcium-bound P (P-HCl) and residual P (P-RES) in the 0–10 mm sediment as well as to P-RES in the 10–20 mm sediment. Results of this work indicate that the Fe-CZ capping has a high potential for the simultaneous management of P and N release from sediments, and the decrease of the contents of sediment P-DGT, sediment P-BD, PORE-water SRP and PORE-water NH_3-N as well as the conversion of mobile P to more stable P in the top sediment should have a significant role in the simultaneous interception of sedimentary P and N liberation into OVER-water by the Fe-CZ capping.

Keywords Sediment · Phosphorus · Nitrogen · Release · Iron-modified calcite/zeolite mixture · Capping · Simultaneous control

Introduction

Eutrophication of freshwater bodies (e.g., lakes, reservoirs, ponds and reservoir type rivers) is a serious global problem resulting from the excess input of nutrient (Moal et al. 2019; Smith et al. 1999; Young et al. 1999; Zhang et al. 2017). Phosphorus (P) and nitrogen (N) have been identified to be the key limiting nutrients responsible for the freshwater eutrophication (Ortiz-Reyes and Anex 2018; Smith et al. 1999). In order to prevent the increase of P and N level in the overlying water (OVER-water) of the freshwater bodies, the control of the discharge of external P and N sources is very necessary. However, the endogenous release of the previously accumulated P and N in sediments may lead to continuous eutrophication in eutrophic freshwater bodies (Liu et al. 2017; Spears et al. 2013; Zhang et al. 2014). Therefore, the interception of sedimentary P and N liberation is of significant importance to prevent the occurrence of the freshwater eutrophication after the control of external P source input.

Several strategies for the control of sedimentary P liberation have been proposed, including dredging (Lürling and Faassen 2012), oxygenation (Yu et al. 2019), chemical precipitation using soluble aluminum salt (Lin et al. 2017), nitrate addition (Wauer et al. 2005), CaO_2 injection (Xu et al. 2018), active capping (Huang et al. 2017; Yin and Kong 2015; Yu

Responsible editor: Tito Roberto Cadaval Jr

✉ Jianwei Lin
jwlin@shou.edu.cn

[1] College of Marine Ecology and Environment, Shanghai Ocean University, Hucheng Huan Road, Pudong District, Shanghai 201306, China

et al. 2018a), and amendment (Meis et al. 2012), etc. Among these methods, the use of P-sorbents as capping or amendment materials for sedimentary P release control in freshwater bodies has received increased attention recently (Copetti et al. 2016; Dithmer et al. 2016; Spears et al. 2013). Several methods have been proposed to control sedimentary N liberation, including dredging (Liu et al. 2017), phytoremediation (Ning et al. 2014), and capping (Xiong et al. 2018; Yin et al. 2018; Zhu et al. 2019), etc. Among them, the use of N-sorbent as a covering material to reduce the internal N loading is considered to be a promising strategy (Xiong et al. 2018, Yin et al. 2018, Zhu et al. 2019).

At present, a lot of capping/amendment materials have been proposed to control P liberation from sediments, including calcite (Berg et al. 2004; Yu et al. 2018b), zeolite (Gu et al. 2019), calcite/zeolite mixture (Lin et al. 2011), bentonite (Gu et al. 2019), iron oxide (Yu et al. 2018b), activated carbon (Bonaglia et al. 2019), lanthanum-activated bentonite (Lürling and Faassen 2012), aluminum-modified zeolite (Gibbs and Özkundakci 2011), zirconium-modified zeolite (Lin et al. 2019b), water treatment sludge (Wang et al. 2013), thermally modified clay (Yin et al. 2016; Yin and Kong 2015), and hydrate silicate calcium (Li et al. 2018; Li et al. 2017a), and so on. Among them, calcite/zeolite mixture has found to have high application potential for the control of P release from sediments (Lin et al. 2011). This is because both calcite and zeolite are naturally available and low-cost, and calcite/zeolite mixture possesses high removal ability for phosphate-P (i.e., soluble reactive P, abbreviated as SRP)(Lin et al. 2011). Additionally, since zeolite exhibits a good adsorption capacity for ammonium (Alshameri et al. 2014; Vocciante et al. 2018) and zeolite capping can reduce the releasing flux of ammonium-N (abbreviated as NH_3-N) from sediments into OVER-water (Huang et al. 2013), sediment capping with calcite/zeolite mixture also could effectively control the release of NH_3-N from sediments into OVER-water (Lin et al. 2011). Thus, calcite/zeolite mixture has high application potential for the simultaneous control of P and N liberation from sediments. However, in order to better apply calcite/zeolite mixture as a capping material to control sedimentary P release, its efficiency still need to be enhanced. This is because the concentration of SRP in OVER-water cannot be controlled at a very low level by the covering layer constructed with calcite/zeolite mixture (Lin et al. 2011), while it can be controlled at a very low level by the capping layer constructed with some synthetic P-sorbet materials such as La-activated bentonite (Wang et al. 2017) and Zr-reacted bentonite (Lin et al. 2019a).

Previous studies showed that iron oxide exhibited excellent affinity with phosphate species in water (Ajmal et al. 2018; Yoon et al. 2014; Zhang et al. 2019). Furthermore, some iron-containing materials such as Fe-based magnetic microparticles (Funes et al. 2016; Funes et al. 2017) and ferrihydrite (Yu et al. 2018b; Zou et al. 2017) have been proposed as capping materials to prevent P liberation from sediments. Therefore, if calcite/zeolite mixture (CZ) is modified by iron, the resultant iron-modified CZ (Fe-CZ) may be a more promising capping material for cutting down the risk of sediment P release than the unmodified CZ. However, little information is available on the simultaneous interception of sedimentary P and N liberation by the Fe-CZ covering layer.

This investigation aimed at evaluating the efficiency of Fe-CZ capping to prevent the liberation of P and N from sediments into OVER-water as well as at determining the mechanism for the control of sedimentary P and N release by capping Fe-CZ. To achieve these aims, the effect of the CZ and Fe-CZ capping layers on the mobilization of P and N in sediments was studied and the impact of sedimentary P release on the P fractionation of the CZ and Fe-CZ capping layers was also investigated. Results of this work will provide solid evidence for the application of Fe-CZ as a covering layer to prevent sedimentary P and N liberation in freshwater bodies.

Materials and methods

Materials

The surface sediment sample used in this research was collected from a semi-closed landscape river in Pudong New Area of Shanghai City, China. The sampled sediments were stored in a bucket and then sieved with a standard 100 mesh for the further use. The original zeolite and calcite used in this work came from Jinyun Country and Changxing Country of Zhejiang province in China, respectively. Prior to the preparation of capping materials, the raw zeolite and calcite were screened through 200 mesh of sieves to make sure that the particle diameter of zeolite and calcite was small than 0.075 mm. All the chemical reagents (analytical reagent grade) used in the experiments were supplied by Sinopharm Chemical Reagent Co., Ltd. (SCRC). All the solutions applied in the experiments were prepared with deionized water (DI-water). The zirconium oxide-based diffusive gradient in thin films (Zr-DGT) probe came from EasySensor limited company.

Preparation of capping materials

The mixture of calcite and zeolite (CZ) was prepared as follows. In brief, 15 g of calcite and 15 g of zeolite were simultaneously added into a 250-mL Erlenmeyer flask, and then 30 mL of DI-water was also introduced into this Erlenmeyer flask. Afterwards, the Erlenmeyer flask was stirred in a shaker at 150 rpm for 1 h. After that, the wet solid was acquired by the centrifugation method at 4000 rpm for 10 min and dried naturally at indoor temperature. At last, the dried CZ was persevered in a sealed plastic bag for later use.

The iron-modified calcite/zeolite mixture (Fe-CZ) was synthesized as follows. Briefly, 2 g of $FeCl_3 \cdot 6H_2O$ was firstly dissolved in 30 mL of DI-water in a 250-mL Erlenmeyer flask. Subsequently, 15 g of calcite and 15 g of zeolite were also added into this Erlenmeyer flask and the mixture was stirred in a shaker at 150 rpm for 1 h. During the agitation process, 1 mol/L of NaOH solution was added dropwise into the Erlenmeyer flask until the solution pH value attained 7.5. Afterwards, the wet solid material was obtained by the centrifugal separation at 4000 rpm for 10 min, washed using DI-water for 3 times and then naturally air-dried at indoor temperature. At last, the dried Fe-CZ was persevered in a sealed plastic bag for later use.

Characterization of capping materials

The X-ray powder diffraction (XRD) patterns of calcite, zeolite and Fe-CZ were taken on a Germany Brucker D8 ADVANCE XRD meter (Cu Kα radiation 40 kV 30 mA, $\lambda = 0.15406$ nm, $2\theta = 5$–$80°$). The elemental compositions of CZ and Fe-CZ were analyzed by a wavelength dispersion X-ray fluorescence (XRF) spectrometer (XRF-1800, Shimadzu, Japan).

Batch P and N sorption experiment

The sorption characteristics of phosphate and ammonium on CZ and Fe-CZ were investigated through batch experiments in a temperature-controlled water bath oscillator at 150 rpm and 298 K. For the study on the effect of contact time on the phosphate removal, 50 mg of CZ and Fe-CZ were added into a series of 100-mL conical flasks containing 50 mL of phosphate solutions with an initial phosphate concentration of 10 mg P/L, respectively, and the mixtures were shaken for various contact time (24, 48, and 72 h). For the study on the influence of initial P concentration on the phosphate removal, 50 mg of CZ and Fe-CZ were added into a series of 100 mL conical flasks containing 50 mL of phosphate solutions with various initial phosphate concentrations (1–10 mg P/L), respectively, and the mixtures were shaken for 24 h. For the ammonium sorption kinetics study, 100 mg of CZ and Fe-CZ were introduced into a series of 50-mL conical flasks containing 25 mL of 10 mg N/L ammonium solution, respectively, and the mixtures were shaken for different contact time (0.5–48 h). For the ammonium sorption isotherm study, 100 mg of CZ and Fe-CZ were added into a series of 50-mL conical flasks containing 25 mL of ammonium solutions with various initial N concentrations (5–40 mg/L), respectively, and the mixtures were shaken for 24 h. The initial pH values of phosphate and ammonium solutions were adjusted with 1 mol/L of NaOH of HCl solution until the value reached 7.5. After reaction equilibrium, the supernatant of mixture solutions was obtained by centrifugation at 4000 rounds per minute for 10 min and filtered through 0.45 μm filter membrane. Subsequently, the standard method, i.e., molybdenum antimony colorimetry and Nessler reagent colorimetry method were applied to determine the residual phosphate-P and ammonium-N concentration in the supernatant liquid on a UV/Vis spectrophotometer at 700 nm. The quantities of phosphate and ammonium removed by CZ and Fe-CZ (q, mg/g) were calculated based on the following equation:

$$q = \frac{V_{RS}}{D_{AM}}(c_I - c_F) \quad (1)$$

where V_{RS} is the volume of phosphate or ammonium reaction solutions (L); D_{AM} is the dosage of sorbent material; c_I and c_F are the concentrations of phosphate or ammonium in solutions before and after sorption, respectively (mg/L).

The pseudo-first-order and pseudo-second-order models (Tran et al. 2017) were applied to analyze the sorption kinetic data, and the Langmuir (Langmuir 1916) and Freundlich (Freundlich 1926) models were used to analyze the sorption isotherm data.

Sediment incubation experiment

The effects of CZ and Fe-CZ capping on the mobilization of P and N in sediments were studied through constructing microcosm sediment incubation experiments. The thoroughly homogenized wet sediments were put into columnar plexiglass reactors (height 40 cm, inner diameter 8.5 cm) until the height of each sediment core reached 5 cm, respectively. Three kinds of sediment columns were designed as follows (Fig. 1): (1) reactor I (control column), the sediment was not subjected to any treatment; (2) reactor II (CZ capping column), 30 g of CZ was homogeneously covered onto the surface of the sediment; (3) reactor III (Fe-CZ capping column), 30 g of Fe-CZ was evenly covered onto the surface of the sediment. The height of capping layer was calculated to be about 4.1 mm.

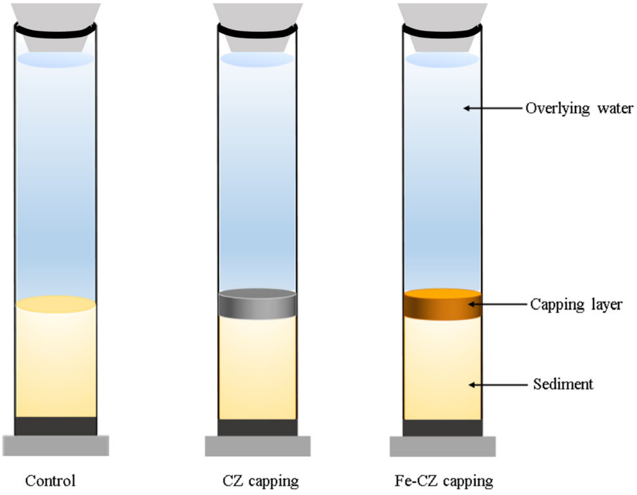

Fig. 1 Schematic diagram of sediment incubation experiments

Subsequently, about 1500 mL of prepared solution, which contained 0.01 mol/L of NaCl, 0.001 mol/L of $CaCl_2$, and 0.001 mol/L of $NaHCO_3$ and had an initial pH value of 7.5, was slowly added into each reactor as OVER-water. After that, each reactor was sealed with rubber stopper and vaseline to prevent air from getting into the reactor. All the sediment reactors were incubated at room temperature for 135 days.

During the incubation period of microcosm sediment experiments, the concentration of DO and the value of pH in OVER-water of each reactor were measured at interval of time. The DO concentration was measured by the use of a HI9143 portable type meter equipped with a DO probe (Hanna Instrument, Romania), and the pH value was determined by the employment of an Orion 320P-01 portable meter equipped with a pH probe (Thermo Corporation, USA). In the meanwhile, 15 mL of OVER-water was sampled from each reactor and the filtration of the sampled water sample was conducted through 0.45 μm filter membrane. Subsequently, the filtered OVER-water was used for the determination of SRP using the molybdenum colorimetry method at 700 nm and NH_3-N using the Nessler reagent colorimetry method at 420 nm, respectively. After each sampling, the equivalent amount of OVER-water was added back into the reactor.

On the 116th day of incubation, the introduction of Zr-DGT probes into the sediment cores was carried out. After 24 h, we took the introduced Zr-DGT probes back from the sediment cores, and the retrieved Zr-DGT probes were cleaned with DI-water until all the sediments on the surface of Zr-DGT probe were fully eliminated. Afterward, the cleaned probe of Zr-DGT was placed into a self-styled bag. Then, the contents of labile P determined by DGT probe (abbreviated as P-DGT) in the OVER-water and sediment profile were analyzed, and the detailed measurement procedure as well as data calculation methods can be seen in the previous literature (Ding et al. 2018).

On the last day of the sediment incubation experiments, the OVER-water in each reactor was removed using the siphon method. After the removal of OVER-water, the capping layer was collected at first, and then the sediments were averagely divided into five parts at 1-cm intervals and collected. In addition, the sediment PORE-water was collected from each part of sediments by the employment of centrifugation and 0.45 μm membrane filtration. After the PORE-water samples were collected, 20 μL of 0.1 mol/L HCl was added into each sample. Then, the concentrations of SRP and NH_3-N in PORE-water were analyzed according to the molybdenum blue at 630 nm of wavelength and Nessler reagent colorimetric methods at 405 nm of wavelength with a BioTek elx800 Epoch Microplate Spectrophotometer (BioTek Instruments, Inc., USA), respectively.

After the analysis of PORE-water finishing, the as-collected wet sediments and capping materials were air dried at room temperature. After that, the amounts of various P species in different sediment layers and capping material layers collected from the control, CZ capping, and Fe-CZ capping columns were measured on the basis of the sequential P fractionation procedure shown in the literatures previously reported (Lin et al. 2019b; Ribeiro et al. 2008; Rydin and Welch 1998). In this procedure, the P in sediments is divided into five forms, namely, easily re-released P (P-LOOSE), redox-sensitive P (P-BD), aluminum-bound P (P-NaOH), calcium-bound P (P-HCl), and residual P (P-RES).

The removal efficiency of SRP or NH_3-N in the water phase (OVER-water and PORE-water) by the capping materials (R, %), i.e., CZ and Fe-CZ, can be calculated according to the following formula:

$$R = \frac{C_{CL} - C_{TR}}{C_{CL}} \times 100\% \tag{2}$$

where C_{CL} and C_{TR} represent the concentrations of SRP or NH_3-N in the water phase including OVER-water and PORE-water of control and treatment sediment reactors, respectively.

Results

Characterization of capping materials

The XRD patterns of calcite, zeolite and Fe-CZ are presented in Fig. 2. It was shown that the main characteristic diffraction peaks of the calcite sample used in this study was attributed to the calcite crystal, which indicates that the calcite sample employed in this research is mainly composed of calcite crystals. The characteristic diffraction peaks of clinoptilolite, mordenite, and quartz were observed in the XRD pattern of zeolite, suggesting that the zeolite sample contains clinoptilolite, mordenite, and quartz. The characteristic diffraction peaks of calcite, clinoptilolite, mordenite, and quartz were found in the XRD pattern of Fe-CZ, demonstrating the presence of calcite, clinoptilolite, mordenite, and quartz in the Fe-CZ sample. This also indicates that the modification of CZ with iron does not change the crystal structure of calcite, clinoptilolite, mordenite, and quartz in the CZ sample. The mass contents (wt%) of elements in CZ and Fe-CZ measured by XRF is listed in Table 1. It was shown that the CZ sample contains a small amount of Fe, which might be due to the presence of Fe-bearing mineral in the zeolite. However, the percentage of Fe in Fe-CZ was much higher than that in CZ. This suggests that the Fe species has been incorporation into Fe-CZ after the modification of CZ with iron. That is to say, the Fe-CZ sample also contains the Fe specie in addition to calcite, clinoptilolite, mordenite, and quartz.

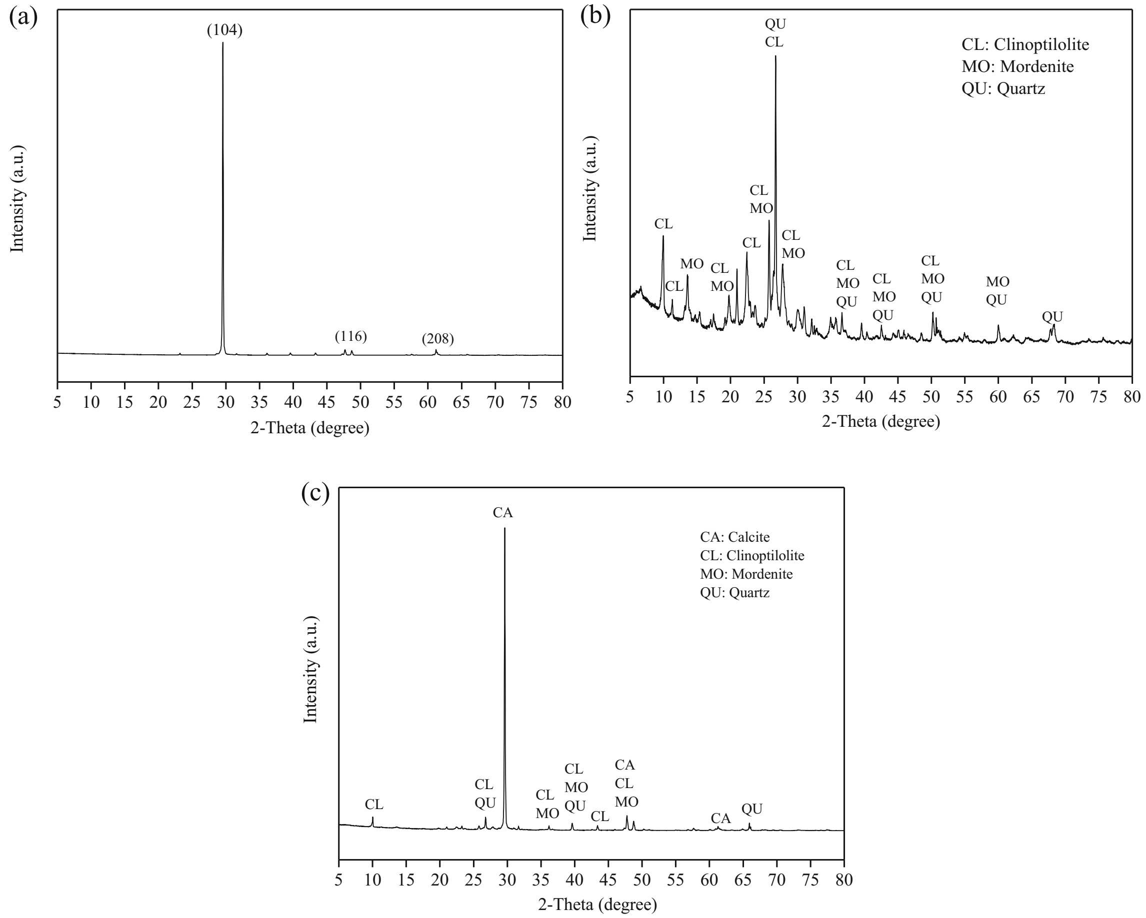

Fig. 2 XRD patterns of **a** calcite, **b** zeolite, and **c** Fe-CZ

Removal of phosphate and ammonium by CZ and Fe-CZ

Figure 3 shows the effect of contact time and initial phosphate concentration on the removal of phosphate by CZ and Fe-CZ. It was observed from Fig. 3a that the amount of phosphate removed by CZ increased from 0.291 to 2.77 mg P/g with the increase of contact time from 1440 to 4320 min, and those by Fe-CZ rose from 1.43 to 6.53 mg P/g as the contact time increased from 1440 to 4320 min. Furthermore, it was found that the quantities of phosphate removed by Fe-CZ under different contact time conditions were much higher those by CZ. As shown in Fig. 3b, the content of phosphate removed by CZ at 1440 min of contact time slightly increased from 0.0666 to 0.0938 mg P/g with the increase of initial phosphate concentration from 1 to 10 mg P/L, but that by Fe-CZ at 1440 min of contact time greatly rose from 0.652 to 1.62 mg P/g with increasing the initial phosphate concentration from 1 to 10 mg P/L. Moreover, the quantities of phosphate removed by Fe-CZ under different initial phosphate concentration conditions were much larger than those by CZ.

Table 1 Mass contents (wt%) of elements in CZ and Fe-CZ measured by XRF

Element	CZ	Fe-CZ
O	83.4	76.2
Na	0.606	0.725
Mg	0.195	0.205
Al	1.67	2.38
Si	5.96	8.63
K	0.233	0.375
Ca	7.76	10.2
Fe	0.0894	0.847
Others	0.0866	0.438

The kinetic data of ammonium sorption onto CZ and Fe-CZ is shown in Fig. 4 a and b, respectively. It was shown that the quantities of ammonium sorbed onto CZ and Fe-CZ significantly increased with increasing contact time in the early stage of sorption and then it gradually increased with the increase of contact time until equilibrium was attained. The calculated parameters of the kinetics models are listed in Table 2. It was shown that the pseudo-second-order model ($R^2 = 0.649$–0.802) fitted better to the kinetic data of ammonium sorption onto CZ and Fe-CZ than the pseudo-first-order model ($R^2 = 0.286$–0.420). The initial ammonium sorption

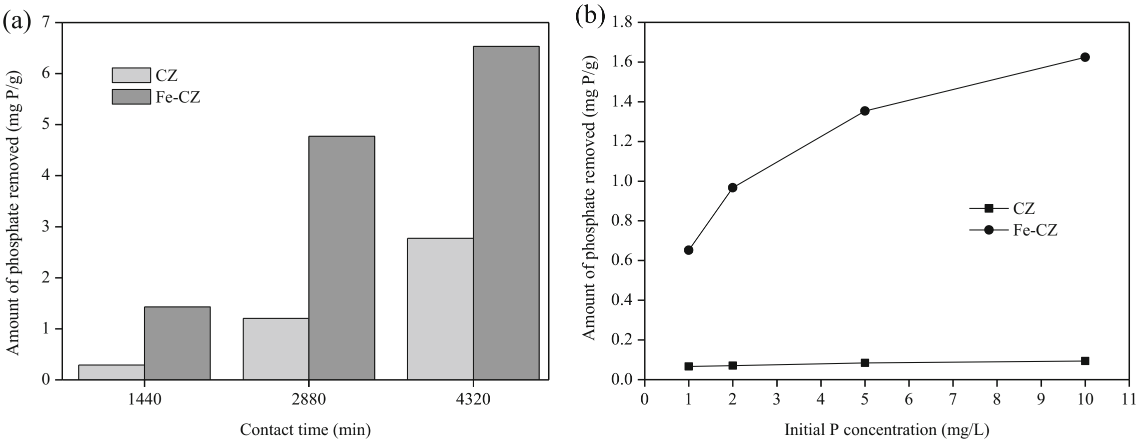

Fig. 3 **a** Effect of contact time on phosphate removal by CZ and Fe-CZ. **b** Impact of initial P concentration on phosphate removal by CZ and Fe-CZ at 24 h of contact time

rates for CZ and Fe-CZ were found to be 0.290 and 0.657 mg/(g min), respectively. The sorption isotherm data of ammonium on CZ and Fe-CZ are presented in Fig. 4 c and d, respectively. The calculated parameters of the isotherm models are also listed in Table 2. According to Table 2, the results suggest that the sorption isotherm data of ammonium onto CZ and Fe-CZ can be better fitted by the Freundlich model ($R^2 = 0.945$ and 0.942, respectively) than the Langmuir model ($R^2 = 0.722$ and 0.650, respectively). The calculated $1/n$ values for ammonium sorption onto CZ and Fe-CZ were 0.284 and 0.235, respectively, which were larger than 0 but less than 1. This demonstrates that the sorption of ammonium on CZ and Fe-CZ is favorable. The predicted value of the maximum ammonium sorption capacities derived from the Langmuir equation for CZ and Fe-CZ were 3.85 and 3.76 mg N/g, respectively, which were close those derived from the batch sorption experiments (3.44 and 3.46 mg N/g, respectively). This means that the prediction of the maximum ammonium sorption

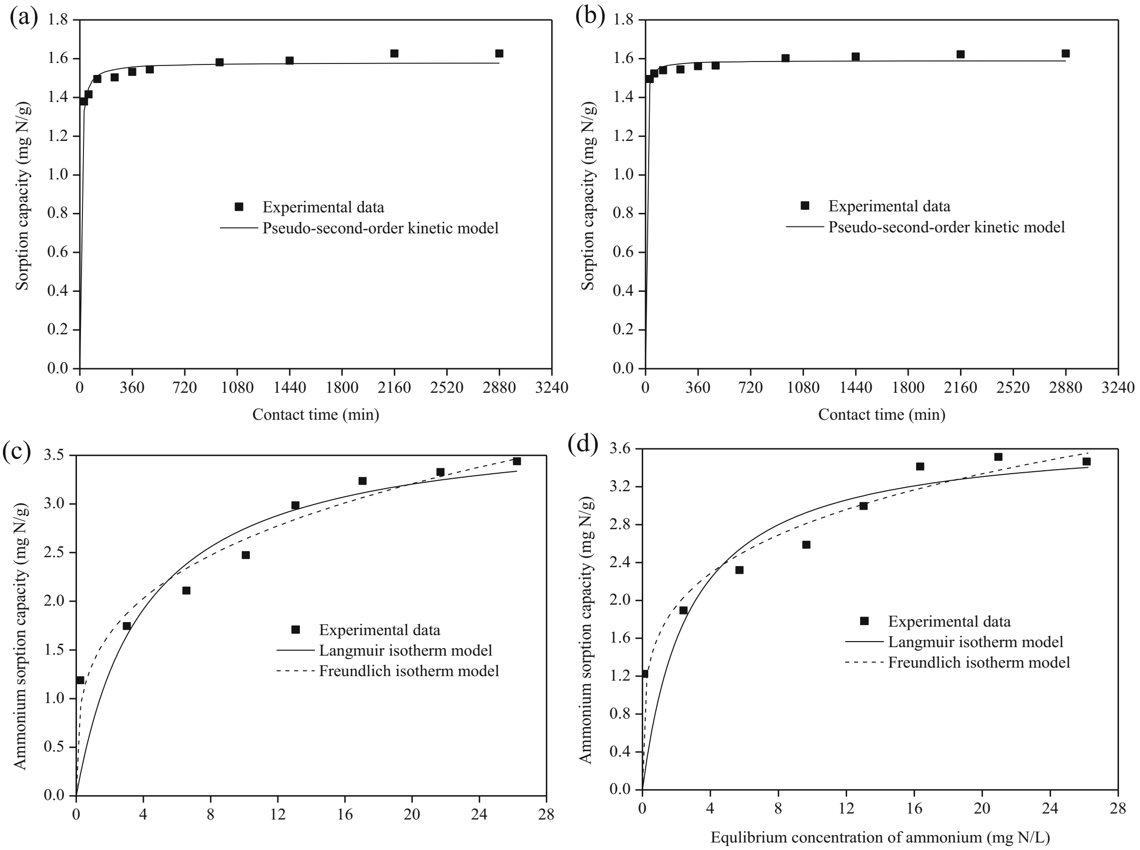

Fig. 4 Sorption kinetics of ammonium on **a** CZ and **b** Fe-CZ; sorption isotherms of ammonium on **c** CZ and **d** Fe-CZ

Table 2 Parameters of kinetic and isotherm models for ammonium sorption onto CZ and Fe-CZ

Models	Parameter	CZ	Fe-CZ
Pseudo-first-order kinetic model $q_t = q_{ES}(1-\exp(-k_1 t))$	$q_{ES,exp}$ (mg/g)	1.63	1.63
	$q_{ES,cal}$ (mg/g)	1.55	1.58
	k_1 (1/min)	0.0679	0.0956
	R^2	0.420	0.286
Pseudo-second-order kinetic model	$q_{ES,exp}$ (mg/g)	1.63	1.63
$q_t = \frac{k_2 q_{ES}^2 t}{1+k_2 q_{ES} t}$	$q_{ES,cal}$ (mg/g)	1.58	1.59
	k_2 (g/(mg min))	0.116	0.260
$v_0 = k_2 q_{ES}^2$	v_0 (mg/(g min))	0.290	0.657
	R^2	0.802	0.649
Langmuir isotherm model $q_{ES} = \frac{q_{MAX} c_{ES} K_{CL}}{1+K_{CL} c_{ES}}$	q_{MAX} (mg/g)	3.85	3.76
	K_{CL} (L/mg)	0.248	0.364
	R^2	0.722	0.650
Freundlich isotherm model $q_{ES} = K_{CF} c_{ES}^{1/n}$	K_{CF}	1.37	1.65
	$1/n$	0.284	0.235
	R^2	0.945	0.942

where t is the contact time (min); q_t and q_{ES} are the contents of sorbate uptake by sorbent at any time t and at state of equilibrium, respectively (mg/g); k_1 (1/min) and k_2 (g/(mg min)) are the rate constants of pseudo-first-order and pseudo-second-order kinetic equations, respectively; v_0 (mg/(g min)) is the initial sorption rate; c_{ES} is the equilibrium concentration of sorbate in aqueous solution (mg/L); q_{MAX} is the maximum monolayer sorbate sorption capacity for sorbent (mg/g); K_{CL} is the constant of Langmuir (L/mg); K_{CF} and $1/n$ are the constants of Freundlich related to the sorption capacity and intensity, respectively

capacity based on the Langmuir isotherm model is reliable. The slight difference of the predicted maximum ammonium sorption capacity between CZ and Fe-CZ indicates that the modification of CZ with iron has a negligible impact on the ammonium uptake ability.

Variation of DO, pH, SRP, and NH_3-N in OVER-water in different columns

The variations of the DO concentrations and pH values of OVER-water in various types of columns with different incubation time are presented in Fig. 5 a and b, respectively. The concentration of DO in the OVER-water of the control column decreased from 3.85 to 0.69 mg/L as the incubation time rose from 5 to 10 days, and afterwards, it varied between 0.16 and 0.69 mg/L with a further augment of the incubation time from 10 to 135 days. This indicates that the sediment in the control is incubated under anoxic condition after 10 days. In the CZ capping column, the OVER-water DO concentration decreased from 4.45 to 0.75 mg/L with increasing the incubation time from 5 to 20 days and then it remained at a low level (0.17–0.95 mg/L) at 20–135 days of the incubation time, demonstrating that the sediment in the CZ capping column is incubated in an anoxic environment after 20 days. For the Fe-CZ covering column, the OVER-water DO concentration declined from 4.28 to 0.78 mg/L when the incubation time rose from 5 to 40 days and after that it was maintained at 0.17–0.78 mg/L at 40–135 days. This suggests the anoxic incubation of the sediment in the Fe-CZ capping column after 40 days. The OVER-water pH values in the control, CZ capping and Fe-CZ capping columns were in the range of 7.14–7.65, 7.16–8.01, and 6.53–7.59, respectively. There was no significant difference of the pH value among the control, CZ capping and Fe-CZ capping columns during the period of the sediment incubation, suggesting that CZ and Fe-CZ capping have a marginal effect on the pH value of OVER-water.

The changes of OVER-water SRP in different columns with incubation time as well as the removal rate of OVER-water by CZ and Fe-CZ capping are presented in Fig. 5 c and d, respectively. It was found that the P concentrations among various columns differed significantly. Without capping, the SRP concentration in OVER-water continuously increased from 0 to 0.882 mg/L in the first 45 days of the incubation experiment, and then decreased to 0.503 mg/L with the further augment of the incubation time to 50 days. After 50 days of incubation, as the incubation experiment went on, the SRP concentration in OVER-water without capping increased again, reaching 0.800 mg/L on the 60th day, and then decreased to 0.247 mg/L on the 65th day. During the period of 65–120 days' incubation, the SRP concentration in OVER-water in the control column slightly varied between 0.247 and

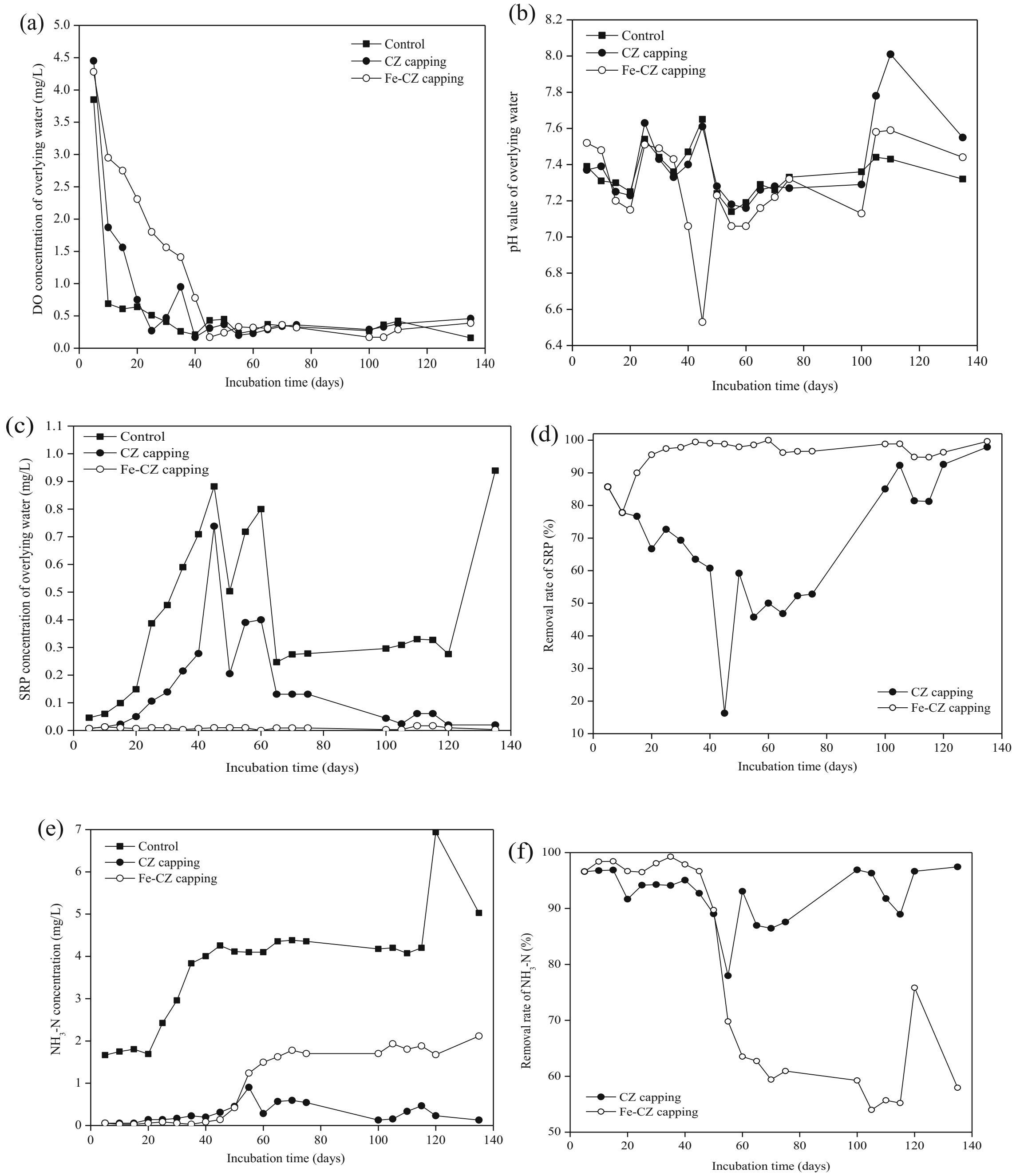

Fig. 5 Variation of **a** DO concentration and **b** pH value of overlying water. **c** Change in SRP concentration of overlying water. **d** Removal rate of SRP in overlying water by capping layers. **e** Change in NH_3-N concentration of overlying water. **f** Removal rate of NH_3-N in overlying water by capping layers

0.330 mg/L. Following this, the SRP concentration showed an increasing trend to 0.939 mg/L by the 135th day. With CZ capping, the SRP concentration in OVER-water gradually rose from 0 to 0.738 mg/L when the incubation time increased from 0 to 45 days, and then slowly decreased until the end of the experiment as a whole. Compared to the control column, the SRP concentrations of OVER-water in the CZ capping column were much less. The reduction rate of OVER-water SRP by the CZ capping layer was found to be 16.3–97.9%. For the Fe-CZ covering column, throughout the period of the sediment incubation, the SRP concentration in OVER-water remained at an extremely low level (0.003–0.017 mg/L). The removal rate of OVER-water SRP by the Fe-CZ capping layer was found to be 77.8–99.7%.

The temporal variations of OVER-water NH_3-N concentration in different columns as well as the removal rate of OVER-water NH_3-N by the CZ and Fe-CZ capping layers are shown in Fig. 5 e and f, respectively. It was shown that the OVER-water NH_3-N concentration without capping increased in the first 45 days of the incubation experiment overall, and then it remained basically unchanged (4.07–4.38 mg/L) with a further increase of the incubation time from 45 to 115 days. After 115 days of incubation, as the incubation experiment went on, the OVER-water NH_3-N concentration without capping increased again, reaching the biggest value of 6.94 mg/L on the 120th day, and afterwards decreased to 5.03 mg/L when the incubation experiment was finished. For the CZ capping column, the concentration of NH_3-N in OVER-water was remained at very low levels (0.13–0.90 mg/L) throughout the whole period of the sediment incubation. The OVER-water NH_3-N concentrations in the CZ capping column were much less than those in the control column, and the removal rates of NH_3-N by the CZ capping layer were found to be 78.0–96.9%. For the Fe-CZ covering column, the NH_3-N concentration in OVER-water remained at very low levels (0.03–0.42 mg/L) in the first 45 days of the experiment, and then increased to 2.14 mg/L at the end of the experiment with the further increase of the incubation time. Compared to the control column, much less concentrations of NH_3-N in OVER-water were observed in the Fe-CZ capping column. The reduction rate of OVER-water NH_3-N by the Fe-CZ capping layer was found to be 54.0–96.7%.

SRP and NH_3-N concentrations in PORE-water

The concentrations of SRP and NH_3-N in the sediment PORE-water at day 135 are depicted in Fig. 6. As can be seen, the concentration of SRP in PORE-water in various columns all steadily increased with the increase of sediment depth. Moreover, the PORE-water SRP concentrations of the 0–30 mm sediment layer in the CZ and Fe-CZ capping columns were less than those in the control column. When the sediment depths were 0–10, 10–20, and 20–30 mm, the reduction rates of PORE-water SRP by the CZ capping layer were calculated to be 38.8, 40.5, and 13.6%, respectively, and those by the Fe-CZ capping layer were calculated to be 77.6, 74.3, and 21.0%, respectively. Obviously, the removal efficiencies of PORE-water SRP at depths of 0–10, 10–20, and 20–30 mm by the Fe-CZ covering layer were higher than those by the CZ covering layer. In general, the concentration of NH_3-N in the sediment PORE-water from the control column increased with the increase of sediment depth. The concentrations of NH_3-N in the sediment PORE-water from the CZ and Fe-CZ capping columns were significantly lower than those from the control column. The CZ capping layer resulted in 57.1, 49.5, 40.9, 50.9, and 24.3% reduction in the concentrations of PORE-water NH_3-N in the 0–10, 10–20, 20–30, 30–40, and 40–50 mm layers sediment, respectively, and the Fe-CZ capping layer led to 23.8, 24.8, 17.4, 39.1, and 38.7% reduction in the PORE-water NH_3-N concentrations in the 0–10, 10–20, 20–30, 30–40, and 40–50 mm sediment layers, respectively.

P-DGT concentrations in overlying water-sediment profiles

The vertical distribution of P-DGT concentration ($C_{\text{P-DGT}}$) in the profile of OVER-water and sediment in different columns is depicted in Fig. 7. A presented in Fig. 7, without capping, the OVER-water $C_{\text{P-DGT}}$ values ranged from 0.099 to 0.135 mg/L, while the $C_{\text{P-DGT}}$ value in the sediment gradually increased from 0.071 to 0.712 mg/L when the depth of sediment increased from 2 to 34 mm. The vertical distribution pattern of $C_{\text{P-DGT}}$ in the CZ and Fe-CZ capping columns was similar to that in the control column. However, the $C_{\text{P-DGT}}$ value in the profile of sediment and OVER-water in the CZ and Fe-CZ capping columns were less than those in the control column. The CZ capping brought about 55.2–91.4% reduction in the $C_{\text{P-DGT}}$ value of OVER-water, and gave rise to 3.0–83.2% reduction in the $C_{\text{P-DGT}}$ value of sediment. The $C_{\text{P-DGT}}$ values of OVER-water in the Fe-CZ covering column

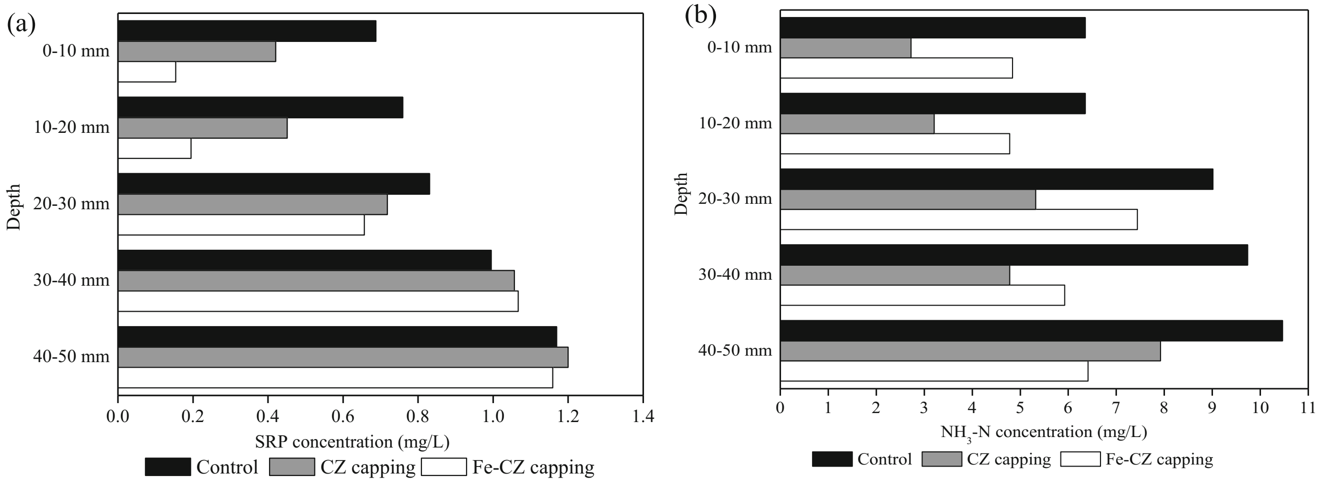

Fig. 6 Impact of CZ and Fe-CZ capping on concentrations of **a** SRP and **b** NH_3-N in PORE-water

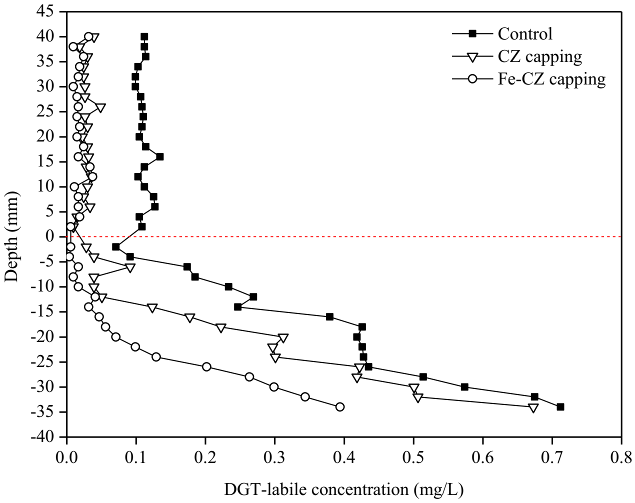

Fig. 7 Influence of CZ and Fe-CZ capping on concentrations of DGT-labile P in overlying water-sediment profile

were 63.6–94.8% less than those in the control column, and those of sediment in the Fe-CZ covering column were 44.6–95.9% lower than those in the control column. Furthermore, the $C_{\text{P-DGT}}$ value in the sediment from the Fe-CZ capping column was less than that from the CZ capping column.

P speciation in sediments

The quantities of various P species in sediments collected from different columns are presented in Fig. 8. It was found that the main P forms of sediments collected from the control, CZ capping and Fe-CZ capping columns were P-BD, P-NaOH, P-HCl, and P-RES, while the sediments from this study contained negligible P-LOOSE. The CZ and Fe-CZ capping gave rise to a significant reduction in the P-BD quantity of sediment. The amounts of P-BD in the sediments at depths of 0–10, 10–20, 20–30, 30–40, and 40–50 mm in the CZ capping column were 50.9, 48.3, 35.1, 37.7, and 27.1% less than those in the control column, respectively, and those in the Fe-CZ capping column were 56.7, 41.7, 39.0, 31.3, and 23.8% lower than those in the control column, respectively. On the whole, the CZ and Fe-CZ capping had little impact on the content of P-NaOH in sediment. After CZ and Fe-CZ capping, the content of P-HCl in the top 10 mm sediment significantly rose (increased by 17.1 and 30.9% after CZ and Fe-CZ capping, respectively), while the P-HCl amount in the 10–50 mm sediment layer did not change remarkably. When comparing the CZ capping column with the control column, the content of P-RES in the top 10 mm sediment increased significantly (by 23.9%), and that in the 10–50 mm sediment layer changed little. The Fe-CZ capping caused an obvious increase in the P-RES quantity of the top 0–20 mm sediment, while it had marginal effect on the amount of P-RES in the 20–50 mm sediment layer.

P fractionation in capping materials after their application

The distribution of various P species in the capping materials collected from the CZ and Fe-CZ columns is illustrated in Fig. 9. It was found that the contents of P-LOOSE, P-BD, P-NaOH, P-HCl, P-RES, and P-TOTAL (total extractable P, sum of P-LOOSE, P-BD, P-NaOH, P-HCl, and P-RES) in the used CZ capping layer were 5.9, 53.1, 17.5, 145.4, 74.8, and 296.7 mg/kg, respectively, while those in the used Fe-CZ capping layer were 2.0, 37.7, 21.8, 177.2, 89.7, and 328.4 mg/kg, respectively. The percentages of various P species to the total adsorbed P in the used CZ covering layer decreased in the order of P-HCl (49.0%) > P-RES (25.2%) > P-BD (17.9%) > P-NaOH (5.9%) > P-LOOSE (2.0%), and those in the used Fe-CZ covering layer decreased in the order of P-HCl (54.0%) > P-RES (27.3%) > P-BD (11.5%) > P-NaOH (6.6%) > P-LOOSE (0.6%).

Discussion

Removal performance and mechanism of phosphate and ammonium by Fe-CZ

Our study found that the sorption equilibrium of ammonium on CZ and Fe-CZ could be easily reached within a short time (Fig. 4 a and b), and the maximum ammonium sorption capacities for CZ and Fe-CZ could reach 3.85 and 3.76 mg N/g, respectively (Table 2). These results indicate that CZ and Fe-CZ give a good performance for ammonium sorption. Previous studies have shown that ammonium sorption onto zeolite is mainly controlled by cation exchange mechanism (Lin et al. 2011; Lin et al. 2014). In addition, calcite has negligible affinity for NH_3-N in water (Lin et al. 2011). Thus, the sorption of NH_3-N from water on CZ is mainly attributed to zeolite, and the cation exchange between zeolite and NH_3-N is a key mechanism responsible for the sorption of NH_3-N from water on CZ. The maximum ammonium sorption capacity for Fe-CZ was close to that for CZ (Table 2), indicating that the modification of CZ with Fe has a slight impact on the sorption capacity for CZ. This also suggests that the sorption of ammonium on Fe-CZ is mainly ascribed to the ammonium sorption ability for CZ rather than Fe species. Thus, similar to CZ, the cation exchange between zeolite and NH_3-N could play a key role in the sorption of ammonium from water on Fe-CZ.

Li et al. (2017b) found that the removal of phosphate by calcite involved adsorption and precipitation mechanisms depending on the initial phosphate concentration and reaction time (Li et al. 2017b). When the initial phosphate concentration was relatively low and the reaction time was relatively short, the removal of phosphate by calcite was mainly governed by adsorption (Li et al. 2017b). When the initial

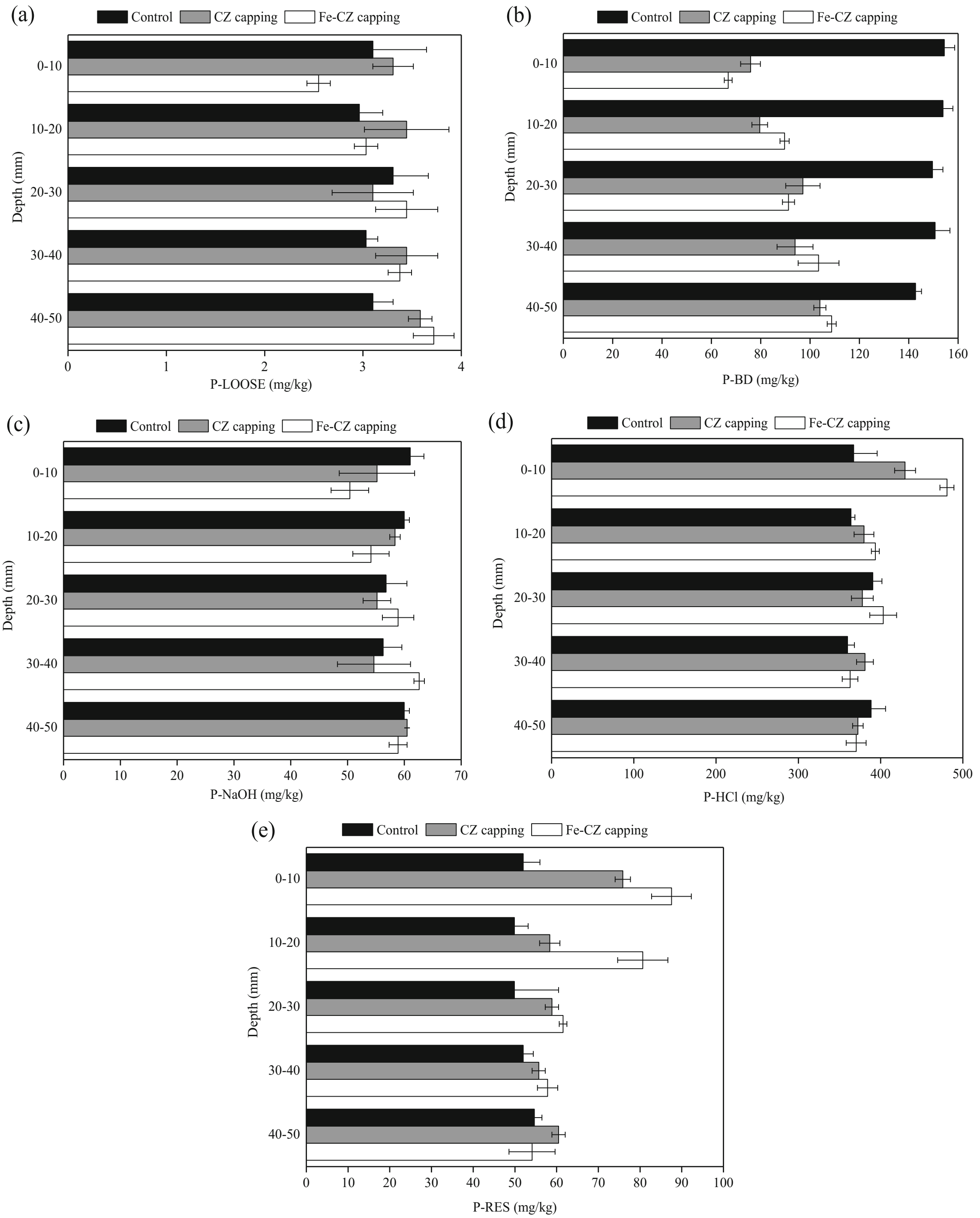

Fig. 8 Effect of CZ and Fe-CZ capping on contents of different P species in sediments including **a** P-LOOSE, **b** P-BD, **c** P-NaOH, **d** P-HCl, and **e** P-RES

phosphate concentration was relatively high and the reaction time was relatively long, the removal of phosphate by calcite started with a certain amount of phosphate adsorption, followed by precipitation (Li et al. 2017b; Liu et al. 2012). Our study found that the amount of phosphate removed by CZ at 1440 min of reaction time was comparatively low (0.291 mg P/g in Fig. 3 a and 0.0666–0.0938 mg P/g in Fig. 3 b), while that at 2880–4320 min of reaction time was comparatively high (1.20–2.77 mg P/g in Fig. 3a). Thus, the adsorption mechanism is expected to play a role in the removal of phosphate by CZ at a relatively short time (e.g., 1440 min), and the precipitation mechanism is expected to play a role in the removal of phosphate by CZ in addition to the adsorption mechanism at a relatively long time (e.g., 2880–4320 min). Additionally, the precipitation of phosphate with the released Ca^{2+} ions from zeolite through a Ca^{2+}/NH_4^+ exchange process

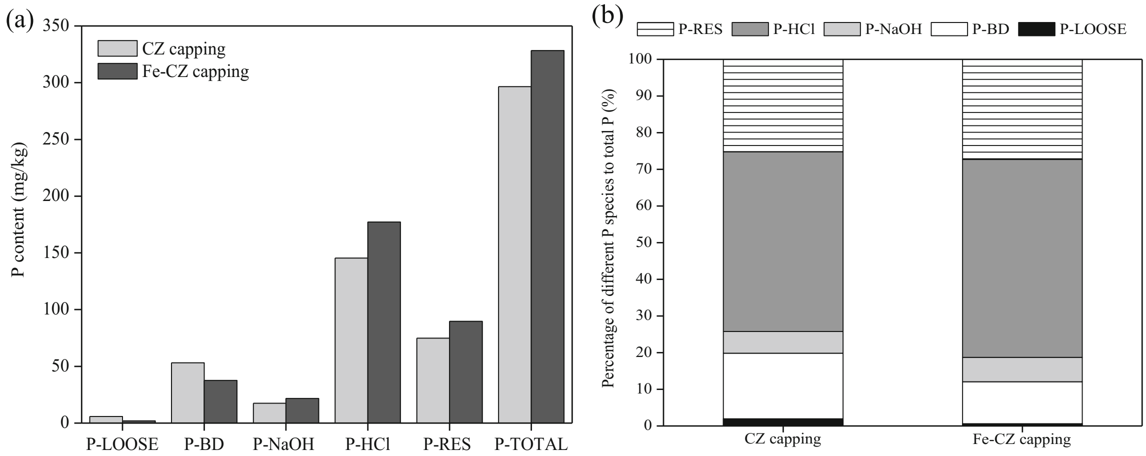

Fig. 9 **a** Contents of different P species in used capping materials. **b** Percentages of various P species to total P in capping materials after their application

was an important mechanism responsible for the removal of phosphate by zeolite (Lin et al. 2011, 2014). Thus, the precipitation of phosphate with the Ca^{2+} ions released from zeolite also plays a role in the removal of phosphate by CZ.

This study found that Fe-CZ presented much higher phosphate sorption capacity than CZ (Fig. 3 a and b), which indicates that Fe-CZ gives a good performance for the phosphate removal. This could be mainly attributed to the strong affinity of Fe species on the Fe-CZ surface towards phosphate. Previous literatures showed that the ligand exchange of hydroxyl groups bound to Fe with the negatively charged oxygen of phosphate forming the inner-sphere Fe-O-P complex is a key mechanism for the absorptive removal of phosphate by iron oxide/hydroxides (Fu et al. 2018; Zhang et al. 2019). Therefore, the mechanisms for the removal of phosphate by Fe-CZ at a relatively long time are expected to include the adsorption of phosphate on calcite, the precipitation of phosphate with the Ca^{2+} ions released from calcite and zeolite, and the adsorption of phosphate on the Fe species of Fe-CZ via a ligand exchange process, while the removal of phosphate by Fe-CZ at a relatively short time are expected to be mainly controlled by the mechanism for the adsorption of phosphate on calcite and Fe species.

Efficiency for control of sedimentary P and N release into OVER-water by Fe-CZ capping layer

When no any capping material was placed onto the top of sediment, the sediment P could be greatly released into the OVER-water under the oxygen-deficient condition, resulting in a high concentration of SRP in the OVER-water under no capping condition (Fig. 5c). This is to say, the sediment used in this study served as a source of P for the water column during the period of the simulation experiment. This could be explained as follows. After 10 days of incubation, the sediment from the control reactor was maintained at the condition of anoxic environment (Fig. 5a). In an aerobic environment, phosphate can reacted with Fe(III) to form $Fe_2(PO_4)_3$ and it can be adsorbed by Fe(III) oxide/hydroxides in sediment, resulting in that it was difficult for the sedimentary P to be released under aerobic condition (Jiang et al. 2008; Kang et al. 2018). In contrast, the anoxic environment could induce the reduction of Fe(III) to Fe(II) and finally result in the liberation of P bound by Fe(III) oxide/hydroxides (Jiang et al. 2008, Kang et al. 2018). Thus, the reductive dissolution of Fe(III) compounds to Fe(II) compounds and the subsequent liberation of P bound to Fe oxide/hydroxide could have an important role in the significant liberation of sediment P in the control reactor after day 10. However, when CZ and Fe-CZ were placed onto the top of sediment, the liberation of P from the sediment into the OVER-water could be effectively intercepted by the CZ and Fe-CZ capping layers, leading to that the concentrations of SRP in the OVER-water under CZ and Fe-CZ covering conditions were much lower than those under no capping condition (Fig. 5c). Furthermore, the concentrations of OVER-water SRP under Fe-CZ capping condition were much less than those under CZ capping condition (Fig. 5c), suggesting that the Fe-CZ capping layer has a stronger ability for intercepting the release of sedimentary P into OVER-water than the CZ capping layer. It is well known that the $C_{\text{P-DGT}}$ value of water is a good indicator representing the labile fraction of P in the water (Burns et al. 2015; Qin et al. 2018; Zhang et al. 1998). After the application of CZ and Fe-CZ as capping materials to cover sediment, the $C_{\text{P-DGT}}$ values in the OVER-water profile greatly decreased (Fig. 7). This further demonstrates that CZ and Fe-CZ capping can effectively control the liberation of P from sediments into OVER-water. It should be noted that the application of Fe-CZ as a capping material decreased the OVER-water SRP concentrations to a very low level (0.003–0.017 mg/L) throughout the whole period of sediment incubation, and a very high controlling efficiency of more than 99% was sustained up to the

135th day after application (Fig. 5 c and d). This indicates that sediment capping with Fe-CZ is a very effective method for the interception of sediment-P release into OVER-water.

Without the placement of capping material on the top of sediment, NH_3-N could be greatly liberated from the sediment into the OVER-water, giving rise to a very high concentration of NH_3-N in the OVER-water under no capping condition (Fig. 5e). In other words, the sediment employed in this research also served as a source of NH_3-N for the water column during the incubation period. However, the liberation of NH_3-N from the sediment into the OVER-water could be effectively intercepted by the CZ and Fe-CZ capping layers, resulting in that the concentrations of NH_3-N in the OVER-water under CZ and Fe-CZ capping conditions were much less than that under no capping condition (Fig. 5e). The application of Fe-CZ as a capping layer decreased the OVER-water NH_3-N concentration to an extremely low level (0.028–0.423 mg/L) during the period of 50 days' incubation, and a very high controlling efficiency of about 90% was sustained up to the 50th day after application (Fig. 5 e and f). Although the controlling efficiency of NH_3-N release from sediment into OVER-water by the Fe-CZ capping layer declined after 50 days, the relatively high controlling efficiency of about 58% was sustained up to the 135th day (Fig. 5 e and f). These results demonstrate that sediment capping with Fe-CZ is an effective method for the control of NH_3-N release from the sediment into the overlying water.

Reduction of PORE-water SRP and NH_3-N by Fe-CZ capping layer

Generally, P and N in sediment are released into PORE-water at first, and the soluble P and N in the PORE-water are then transported into OVER-water via a diffusion mechanism (Yu et al. 2017; Zhu et al. 2019). That is to say, the molecular diffusion of the dissolved P and N from PORE-water to OVER-water at the interface between the OVER-water and sediment (IF-SW) is an important way for the liberation of sedimentary P and N into OVER-water. According to the diffusion theory, the diffusion flux of the dissolved P and N from PORE-water into OVER-water across the IF-SW depends on the concentration difference of the dissolved P and N between PORE-water and OVER-water, and a high level of the soluble P and N in PORE-water is beneficial to the upward diffusion of the dissolved P and N from PORE-water into OVER-water (Yu et al. 2017, Zhu et al. 2019). Thus, if the soluble P and N in PORE-water are removed by the capping material, the risk of the diffusion of the dissolved P and N from PORE-water into OVER-water will be reduced, which will be conducive to the interception of sedimentary P and N liberation by the capping material. Our study found that the concentration of PORE-water SRP in the 0–20 mm sediment layer and that of PORE-water NH_3-N in the 0–50 mm sediment layer were greatly reduced by the CZ and Fe-CZ capping layers (Fig. 6), weakening the free molecular diffusion of SRP and NH_3-N from PORE-water to OVER-water through the IF-SW. Thus, the reductions of PORE-water SRP and NH_3-N concentrations after capping CZ and Fe-CZ play an important role in the prevention of sedimentary P and N release into OVER-water by the CZ and Fe-CZ capping.

This work found that CZ and Fe-CZ possessed a good ability to remove phosphate and ammonium from aqueous solution (Fig. 3, Fig. 4 and Table 2). Therefore, the reduction of SRP and NH_3-N in PORE-water after CZ and Fe-CZ capping (Fig. 6) could be mainly attributed to the immobilization of PORE-water SRP and NH_3-N by the CZ and Fe-CZ capping layers. The immobilization of NH_3-N in PORE-water by the CZ and Fe-CZ capping layers could be mainly attributed to zeolite, and the cation exchange reaction between zeolite and NH_3-N could be a key mechanism responsible for the immobilization of NH_3-N from PORE-water by the CZ and Fe-CZ capping layers. The immobilization of SRP in PORE-water by the CZ capping layer could be mainly controlled by adsorption and precipitation mechanisms, that is to say, the adsorption of SRP on calcite and the precipitation of SRP with the Ca^{2+} ions that was released from calcite and zeolite. The immobilization of SRP in PORE-water by the Fe-CZ capping layer could be mainly ascribed to the adsorption of SRP on calcite, the precipitation of phosphate with Ca^{2+} released from calcite and zeolite, and the adsorption of SRP on the Fe species of Fe-CZ via a ligand exchange process.

Stratification of P-DGT in sediment after Fe-CZ capping

P-DGT in sediment not only includes the labile fraction in PORE-water but also includes the labile fraction being weakly linked to the sediment solid (Chen et al. 2015; Ding et al. 2015). Thus, the $C_{\text{P-DGT}}$ value of sediments is a good indicator that can reflect the risk of P release from the sediment solids into the water phase including PORE-water and OVER-water. In the present study, sediment capping with CZ and Fe-CZ both caused the reduction of P-DGT in the sediment (Fig. 7). This indicates that the CZ and Fe-CZ capping both increases the difficulty of the release of sedimentary P into PORE-water. Obviously, the decrease of the risk of P release from sediments into PORE-waters is beneficial to the interception of sedimentary P liberation into OVER-waters. In addition, this work showed that the reduction efficiency of P-DGT in sediments by the Fe-CZ capping layer was higher than that by the CZ capping layer (Fig. 7). This demonstrates that the difficulty of P release from sediments into PORE-waters under Fe-CZ capping condition is larger than that under CZ capping condition. Thus, from the point of the view of the reduction in the sediment P-DGT concentration, Fe-CZ capping is a better option for inhibiting the liberation of P from sediments than CZ capping. Previous studies (Ding et al. 2018; Lin et al. 2019b; Wang et al. 2017) found that the $C_{\text{P-DGT}}$ value of the sediment directly below the IF-SW at a certain depth was tremendously reduced by capping with lanthanum-activated bentonite (Phoslock®) and zirconium-modified bentonite (ZMB), and a static layer with an extremely low $C_{\text{P-DGT}}$ was formed in the top sediment layer directly below the IF-SW. These previous studies (Ding et al. 2018, Lin et al. 2019b, Wang et al. 2017) also found that the formation of static layer in the upper sediment plays a key role in the prevention of sedimentary P liberation into OVER-water. In this study, after Fe-CZ capping, a very low concentration of P-DGT (0.004–0.017 mg/L) was found in the 0–10 mm sediment layer. This suggests the formation of P static layer in the 0–10 mm sediment layer after Fe-CZ capping. Thus, the appearance of P static layer in the 0–10 mm sediment layer is critical to sustaining the capping effect of Fe-CZ.

Effect of Fe-CZ capping on P speciation in sediments

The stabilization of P in sediments is closely associated to its speciation. It is commonly accepted that P-LOOSE and P-BD are easy to be liberated under common pH and anoxic condition, and they are the components of mobile P in sediments becoming the internal source of P (Meis et al. 2012; Rydin and Welch 1998; Wang and Pei 2013). To be contrary, P-NaOH and P-HCl are relatively stable and are difficulty released under common pH and anoxic condition (Meis et al. 2012; Wang and Pei 2013). P-RES is very stable form of P in sediment and is very difficult to be liberated from sediment (Meis et al. 2012). In the present study, the CZ and Fe-CZ capping gave rise to a significant decrease in the quantity of P-BD in the 0–50-mm sediment layer, while it had a marginal influence on the P-LOOSE amount in the 0–50-mm sediment layer (Fig. 8), indicating that the quantity of mobile P in the sediment can be effectively reduced by the CZ and Fe-CZ capping layers. Furthermore, the CZ and Fe-CZ capping had little influence on the P-NaOH concatenation in the 0–10-mm sediment layer, but increased the amounts of P-HCl and P-RES in the 0–10-mm sediment layer (Fig. 8). This suggests that the CZ and Fe-CZ capping can induce the transformation of P-BD to P-HCl and P-RES in the top 10 mm sediment. Moreover, the CZ and Fe-CZ capping had little impact on the P-NaOH and P-HCl amounts in the 10–20 mm sediment, and the CZ capping also had negligible effect on the P-RES content in the 10–20 mm sediment. But, the Fe-CZ capping increased the P-RES content in the 10–20 mm sediment. This demonstrates that the Fe-CZ capping also can induce the conversion of P-BD to P-RES in the 10–20 mm sediment. In addition, the CZ and Fe-CZ capping had a small influence on the contents of P-NaOH, P-HCl, and P-RES in the 20–50 mm sediment. This implies that the main reason for the disappearing of P-BD in the 20–50 mm sediment is the upward transportation of P-BD towards the 0–20-mm sediment layer or the capping layer.

Taking all the above results and discussion into account, the explanation for the reduction of mobile P in the upper sediment after CZ and Fe-CZ capping were proposed. Under CZ and Fe-CZ capping condition, the mobile P in sediment could be released into PORE-water at first, and then the dissolved P in PORE-water could be effectively sorbed by the CZ and Fe-CZ capping layers. The CZ and Fe-CZ capping could accelerate the liberation of mobile P from sediment into PORE-water, which could be resulted in the reduction of mobile P in the sediment after CZ and Fe-CZ capping compared to no capping. Additionally, the change of P-BD to other forms of P (P-HCl and P-RES) is also responsible for the reduction of in the top sediment layer by the CZ and Fe-CZ capping layers.

P accumulation in Fe-CZ capping layer after application and stabilization of P in used Fe-CZ capping layer

If the P bound by the capping material is unstable and easy to be re-released, the control efficiency of sedimentary P liberation by the capping material is expected to be low. In this investigation, the contents of P-TOTAL in the used CZ and Fe-CZ were 297 and 328 mg/kg, respectively (Fig. 9a). This result indicates that the CZ and Fe-CZ capping layers can effectively adsorb the P in the system of sediment and water. Furthermore, the amount of P-TOTAL in the used Fe-CZ was higher than that in the used CZ, which suggests that Fe-CZ has a strong ability for the sorption of P from the sediment-water system. Moreover, the percentages of mobile P (sum of P-LOOSE and P-BD) in the used CZ and Fe-CZ capping layers were 19.9 and 12.1%, respectively, while those of non-mobile P (sum of P-NaOH, P-HCl and P-RES) were 80.1 and 87.9%, respectively (Fig. 9b). This suggests that most of the P bound by the CZ and Fe-CZ capping layers is relatively or very stable, and most of the bound P is difficult to be re-released into OVER-water under common pH (5–9) and anoxic condition. Thus, form the point of view of the stability of the bound P in the capping layer as well as the sorption efficiency of P from the sediment-water system, CZ and Fe-CZ are suitably used as covering materials for the interception of sedimentary P liberation, and Fe-CZ capping is a better choice for the control of P liberation from sediments.

Mechanism for control of sedimentary P and N liberation by Fe-CZ capping

From the results and discussion mentioned above, the mechanism for the interception of sedimentary P and N liberation into OVER-water by capping Fe-CZ is proposed. Without Fe-CZ capping, P and N could be released from sediment into

PORE-water firstly, and then the soluble P and N in PORE-water could be further transported into OVER-water through the IF-SW via a diffusion mechanism. Under Fe-CZ capping condition, the capping layer could induce the transformation of mobile P (mainly P-BD) to non-mobile P (mainly P-HCl and P-RES) in the top sediment, which makes the P in the top sediment more stable relative to no capping. This will increase the difficulty of the liberation of P from the top sediment into PORE-water, which will be beneficial for the control of P liberation from sediments by capping Fe-CZ. Furthermore, the P and N in PORE-water could be diffused towards the Fe-CZ capping layer. Once the soluble P and N arrived at the Fe-CZ capping layer, they will be immobilized by the Fe-CZ capping layer, giving rise to the decrease of the SRP, P-DGT, and NH_3-N concentrations as well as the formation of P static layer in the upper sediment. This also will make a contribution to the interception of sedimentary P and N liberation by capping Fe-CZ.

Conclusion

Based on the results of this research, the following conclusion can be made:

1. Sediment capping with Fe-CZ not only gave rise a significant reduction of OVER-water SRP and NH_3-N concentrations, but also brought about a great decrease of PORE-water SRP concentration in the 0–30-mm sediment layer as well as PORE-water NH_3-N concentration in the 0–50-mm sediment layer.
2. The Fe-CZ capping layer gave rise to a great decrement of P-DGT in the profile of OVER-water and sediment.
3. The Fe-CZ capping resulted in the reduction of P-BD in the top 50 mm sediment, and caused the transformation of P-BD to P-HCl and P-RES in the top 10 mm sediment as well as the conversion of P-BD to P-RES in the 10–20 mm sediment.
4. Most of the P bound by the Fe-CZ capping layer is relatively or very stable, and it is difficult to be re-released into OVER-water under common pH (5–9) and anoxic condition.
5. The reduction efficiencies of the OVER-water SRP, the PORE-water SRP at depth of 0–30 mm, the OVER-water P-DGT and the P-DGT of the top 35 mm sediment by the Fe-CZ capping layer were higher than those by the CZ capping layer.

Results of this research indicate that the Fe-CZ capping has a high potential for the simultaneous management of P and N release from sediments, and the decrease of sediment P-DGT, PORE-water SRP and PORE-water NH_3-N as well as the transformation of mobile P to more stable P after Fe-CZ capping should have a significant role in the simultaneous interception of sedimentary P and N liberation into OVER-water by capping Fe-CZ.

Acknowledgments This research was financially supported by the Shandong Key Scientific and Technical Innovation Project (2018YFJH0902), the Shanghai Natural Science Foundation (15ZR1420700), the National Science Foundation of China (50908142 and 51408354), and the Scientific Research Project of Shanghai Science and Technology Committee (10230502900).

References

Ajmal Z, Muhmooda A, Usman M, Kizito S, Lu JX, Dong RJ, Wu SB (2018) Phosphate removal from aqueous solution using iron oxides: adsorption, desorption and regeneration characteristics. J Colloid Interface Sci 528:145–155

Alshameri A, Ibrahim A, Assabri AM, Lei X, Wang H, Yan C (2014) The investigation into the ammonium removal performance of Yemeni natural zeolite: modification, ion exchange mechanism, and thermodynamics. Powder Technol 258:20–31

Berg U, Neumann T, Donnert D, Nüesch R, Stüben D (2004) Sediment capping in eutrophic lakes-efficiency of undisturbed calcite barriers to immobilize phosphorus. Appl Geochem 19:1759–1771

Bonaglia S, Rämö R, Marzocchi U, Le Bouille L, Leermakers M, Nascimento FJA, Gunnarsson JS (2019) Capping with activated carbon reduces nutrient fluxes, denitrification and meiofauna in contaminated sediments. Water Res 148:515–525

Burns EE, Comber S, Blake W, Goddard R, Couldrick L (2015) Determining riverine sediment storage mechanisms of biologically reactive phosphorus in situ using DGT. Environ. Sci. Pollut. R. 22: 9816–9828

Chen M, Ding S, Liu L, Xu D, Han C, Zhang C (2015) Iron-coupled inactivation of phosphorus in sediments by macrozoobenthos (chironomid larvae) bioturbation: evidences from high-resolution dynamic measurements. Environ Pollut 204:241–247

Copetti D, Finsterle K, Marziali L, Stefani F, Tartari G, Douglas G, Reitzel K, Spears BM, Winfield IJ, Crosa G, D'Haese P, Yasseri S, Lürling M (2016) Eutrophication management in surface waters using lanthanum modified bentonite: a review. Water Res 97:162–174

Ding SM, Han C, Wang YP, Yao L, Wang YY, Xu D, Sun Q, Williams PN, Zhang CS (2015) In situ, high-resolution imaging of labile phosphorus in sediments of a large eutrophic lake. Water Res 74: 100–109

Ding SM, Sun Q, Chen X, Liu Q, Wang D, Lin J, Zhang CS, Tsang DCW (2018) Synergistic adsorption of phosphorus by iron in lanthanum modified bentonite (Phoslock®): new insight into sediment phosphorus immobilization. Water Res 134:32–43

Dithmer L, Nielsen UG, Lürling M, Spears BM, Yasseri S, Lundberg D, Moore A, Jensen ND, Reitzel K (2016) Responses in sediment phosphorus and lanthanum concentrations and composition across 10 lakes following applications of lanthanum modified bentonite. Water Res 97:101–110

Freundlich H (1926) Colloid and capillary chemistry. Methuen, London

Fu H, Yang Y, Zhu R, Liu J, Usman M, Chen Q, He H (2018) Superior adsorption of phosphate by ferrihydrite-coated and lanthanum-decorated magnetite. J Colloid Interface Sci 530:704–713

Funes A, de Vicente J, Cruz-Pizarro L, Álvarez-Manzaneda I, de Vicente I (2016) Magnetic microparticles as a new tool for lake restoration: a microcosm experiment for evaluating the impact on phosphorus fluxes and sedimentary phosphorus pools. Water Res 89:366–374

Funes A, del Arco A, Álvarez-Manzaneda I, de Vicente J, de Vicente I (2017) A microcosm experiment to determine the consequences of magnetic microparticles application on water quality and sediment phosphorus pools. Sci Total Environ 579:245–253

Gibbs M, Özkundakci D (2011) Effects of a modified zeolite on P and N processes and fluxes across the lake sediment–water interface using core incubations. Hydrobiologia 661:21–35

Gu BW, Hong SH, Lee CG, Park SJ (2019) The feasibility of using bentonite, illite, and zeolite as capping materials to stabilize nutrients and interrupt their release from contaminated lake sediments. Chemosphere 219:217–226

Huang T, Zhou Z, Su J, Dong Y, Wang G (2013) Nitrogen reduction in a eutrophic river canal using bioactive multilayer capping (BMC) with biozeolite and sand. J Soils Sediments 13:1309–1317

Huang XJ, Shi WH, Ni JP, Li ZL (2017) Evaluation of laboratory-scale in situ capping sediments with purple parent rock to control the eutrophication. Environ Sci Pollut R 24:7114–7123

Jiang X, Jin XC, Yao Y, Li LH, Wu FC (2008) Effects of biological activity, light, temperature and oxygen on phosphorus release processes at the sediment and water interface of Taihu Lake, China. Water Res 42:2251–2259

Kang MX, Peng S, Tian YM, Zhang HY (2018) Effects of dissolved oxygen and nutrient loading on phosphorus fluxes at the sediment–water interface in the Hai River Estuary, China. Mar Pollut Bull 130:132–139

Langmuir I (1916) The constitution and fundamental properties of solids and liquids part I. Solid J Am Chem Soc 38:2221–2295

Li CJ, Yu HX, Tabassum S, Li LF, Wu DY, Zhang ZJ, Kong HN, Xu P (2017a) Effect of calcium silicate hydrates (CSH) on phosphorus immobilization and speciation in shallow lake sediment. Chem Eng J 317:844–853

Li Z, Sun X, Huang L, Liu D, Yu L, Wu H, Wei D (2017b) Phosphate adsorption and precipitation on calcite under calco-carbonic equilibrium condition. Chemosphere 183:419–428

Li CJ, Yu HX, Tabassum S, Li LF, Mu YL, Wu DY, Zhang ZJ, Kong HN, Xu P (2018) Effect of calcium silicate hydrates coupled with Myriophyllum spicatum on phosphorus release and immobilization in shallow lake sediment. Chem Eng J 331:462–470

Lin JW, Zhan YH, Zhu ZL (2011) Evaluation of sediment capping with active barrier systems (ABS) using calcite/zeolite mixtures to simultaneously manage phosphorus and ammonium release. Sci Total Environ 409:638–646

Lin L, Wan CL, Lee D-J, Lei ZF, Liu X (2014) Ammonium assists orthophosphate removal from high-strength wastewaters by natural zeolite. Sep Purif Technol 133:351–356

Lin J, Sun Q, Ding SM, Wang D, Wang Y, Chen MS, Shi L, Fan XF, Tsang DCW (2017) Mobile phosphorus stratification in sediments by aluminum immobilization. Chemosphere 186:644–651

Lin J, He S, Zhan Y, Zhang Z, Wu X, Yu Y, Zhao Y, Wang Y (2019a) Assessment of sediment capping with zirconium-modified bentonite to intercept phosphorus release from sediments. Environ. Sci. Pollut. R. 26:3501–3516

Lin JW, He SQ, Zhang HH, Zhan YH, Zhang ZB (2019b) Effect of zirconium-modified zeolite addition on phosphorus mobilization in sediments. Sci Total Environ 646:144–157

Liu Y, Sheng X, Dong YH, Ma YJ (2012) Removal of high-concentration phosphate by calcite: effect of sulfate and pH. Desalination 289:66–71

Liu C, Chen K, Wang Z, Fan C, Gu X, Huang W (2017) Nitrogen exchange across the sediment-water interface after dredging: the influence of contaminated riverine suspended particulate matter. Environ Pollut 229:879–886

Lürling M, Faassen EJ (2012) Controlling toxic cyanobacteria: effects of dredging and phosphorus-binding clay on cyanobacteria and microcystins. Water Res 46:1447–1459

Meis S, Spears BM, Maberly SC, O'Malley MB, Perkins RG (2012) Sediment amendment with Phoslock® in Clatto Reservoir (Dundee, UK): investigating changes in sediment elemental composition and phosphorus fractionation. J Environ Manag 93:185–193

Moal ML, Gascuel-Odoux C, Ménesguen A, Souchon Y, Étrillard C, Levain A, Moatar F, Pannard A, Souchu P, Lefebvre A, Pinay G (2019) Eutrophication: a new wine in an old bottle? Sci Total Environ 651:1–11

Ning D, Huang Y, Pan R, Wang F, Wang H (2014) Effect of eco-remediation using planted floating bed system on nutrients and heavy metals in urban river water and sediment: a field study in China. Sci Total Environ 485-486:596–603

Ortiz-Reyes E, Anex RP (2018) A life cycle impact assessment method for freshwater eutrophication due to the transport of phosphorus from agricultural production. J Clean Prod 177:474–482

Qin W, Gu Y, Wang G, Wu T, Zhang H, Tang X, Zhang Y, Zhao H (2018) Zirconium metal organic frameworks-based DGT technique for in situ measurement of dissolved reactive phosphorus in waters. Water Res 147:223–232

Ribeiro DC, Martins G, Nogueira R, Cruz JV, Brito AG (2008) Phosphorus fractionation in volcanic lake sediments (Azores – Portugal). Chemosphere 70:1256–1263

Rydin E, Welch EB (1998) Aluminum dose required to inactivate phosphate in lake sediments. Water Res 32:2969–2976

Smith VH, Tilman GD, Nekola JC (1999) Eutrophication: impacts of excess nutrient inputs on freshwater, marine, and terrestrial ecosystems. Environ Pollut 100:179–196

Spears BM, Meis S, Anderson A, Kellou M (2013) Comparison of phosphorus (P) removal properties of materials proposed for the control of sediment P release in UK lakes. Sci Total Environ 442:103–110

Tran HN, You SJ, Hosseini-Bandegharaei A, Chao HP (2017) Mistakes and inconsistencies regarding adsorption of contaminants from aqueous solutions: a critical review. Water Res 120:88–116

Vocciante M, De Folly D'AA, Finocchi A, Tagliabue M, Bellettato M, Ferrucci A, Reverberi AP, Ferro S (2018) Adsorption of ammonium on clinoptilolite in presence of competing cations: investigation on groundwater remediation. J Clean Prod 198:480–487

Wang CH, Pei YS (2013) Effects of light, microbial activity, and sediment resuspension on the phosphorus immobilization capability of drinking water treatment residuals in lake sediment. Environ. Sci. Pollut. R. 20:8900–8908

Wang CH, Liu JF, Pei YS (2013) Effect of hydrogen sulfide on phosphorus lability in lake sediments amended with drinking water treatment residuals. Chemosphere 91:1344–1348

Wang Y, Ding SM, Wang D, Sun Q, Lin J, Shi L, Chen MS, Zhang CS (2017) Static layer: a key to immobilization of phosphorus in sediments amended with lanthanum modified bentonite (Phoslock®). Chem Eng J 325:49–58

Wauer G, Gonsiorczyk T, Kretschmer K, Casper P, Koschel R (2005) Sediment treatment with a nitrate-storing compound to reduce phosphorus release. Water Res 39:494–500

Xiong CH, Wang DY, Tam NF, Dai YY, Zhang XM, Tang XY, Yang Y (2018) Enhancement of active thin-layer capping with natural zeolite to simultaneously inhibit nutrient and heavy metal release from sediments. Ecol Eng 119:64–72

Xu Y, F-e H, D-p L, Zhou J, Huang Y (2018) Transformation of internal sedimentary phosphorus fractions by point injection of CaO_2. Chem Eng J 343:408–415

Yin H, Kong M (2015) Reduction of sediment internal P-loading from eutrophic lakes using thermally modified calcium-rich attapulgite-based thin-layer cap. J Environ Manag 151:178–185

Yin H, Han M, Tang W (2016) Phosphorus sorption and supply from eutrophic lake sediment amended with thermally-treated calcium-rich attapulgite and a safety evaluation. Chem Eng J 285:671–678

Yin H, Zhu J, Tang W (2018) Management of nitrogen and phosphorus internal loading from polluted river sediment using Phoslock® and modified zeolite with intensive tubificid oligochaetes bioturbation. Chem Eng J 353:46–55

Yoon S-Y, Lee C-G, Park J-A, Kim J-H, Kim S-B, Lee S-H, Choi J-W (2014) Kinetic, equilibrium and thermodynamic studies for phosphate adsorption to magnetic iron oxide nanoparticles. Chem Eng J 236:341–347

Young K, Morse GK, Scrimshaw MD, Kinniburgh JH, MacLeod CL, Lester JN (1999) The relation between phosphorus and eutrophication in the Thames catchment, UK. Sci Total Environ 228:157–183

Yu JH, Ding SM, Zhong JC, Fan CX, Chen QW, Yin HB, Zhang L, Zhang YL (2017) Evaluation of simulated dredging to control internal phosphorus release from sediments: focused on phosphorus transfer and resupply across the sediment-water interface. Sci Total Environ 592:662–673

Yu JH, Zhong JC, Chen QW, Huang W, Hu LM, Zhang YL, Fan CX (2018a) An investigation of the effects of capping on internal phosphorus release from sediments under rooted macrophytes (Phragmites australis) revegetation. Environ Sci Pollut R 25: 24682–24694

Yu XF, Grace MR, Sun GZ, Zou YC (2018b) Application of ferrihydrite and calcite as composite sediment capping materials in a eutrophic lake. J Soils Sediments 18:1185–1193

Yu P, Wang J, Chen J, Guo J, Yang H, Chen Q (2019) Successful control of phosphorus release from sediments using oxygen nano-bubble-modified minerals. Sci Total Environ 663:654–661

Zhang H, Davison W, Gadi R, Kobayashi T (1998) In situ measurement of dissolved phosphorus in natural waters using DGT. Anal Chim Acta 370:29–38

Zhang L, Wang S, Wu Z (2014) Coupling effect of pH and dissolved oxygen in water column on nitrogen release at water–sediment interface of Erhai Lake, China. Estuar Coast Shelf S 149:178–186

Zhang W, Jin X, Liu D, Lang C, Shan B (2017) Temporal and spatial variation of nitrogen and phosphorus and eutrophication assessment for a typical arid river — Fuyang River in northern China. J Environ Sci 55:41–48

Zhang H, Elskens M, Chen G, Chou L (2019) Phosphate adsorption on hydrous ferric oxide (HFO) at different salinities and pHs. Chemosphere 225:352–359

Zhu YY, Tang WZ, Jin X, Shan BQ (2019) Using biochar capping to reduce nitrogen release from sediments in eutrophic lakes. Sci Total Environ 646:93–104

Zou YC, Grace MR, Roberts KL, Yu XF (2017) Thin ferrihydrite sediment capping sequestrates phosphorus experiencing redox conditions in a shallow temperate lacustrine wetland. Chemosphere 185: 673–680